SEISMIC EVALUATION OF OLD RC WAFFLE FLAT-PLATE SYSTEMS

X. Cahís [1], A. Benavent-Climent [2] and A. Catalan [3]

[1] *Associate Professor, University of Girona, Spain*
[2] *Associate Professor, University of Granada, Spain*
[3] *Associate Professor, University of Oviedo, Spain*

Email: xavier.cahis@udg.edu

ABSTRACT :

In moderate-seismicity southern European countries it is very common to use reinforced concrete waffle flat-plate structures for sustaining both vertical and lateral earthquake loads. In the case of Spain, many of these structures were designed during the seventies, eighties and nineties according to earlier seismic codes which required relatively small lateral strength and did not contain any provision for attaining ductility. Past earthquakes have raised serious concerns about the safety of these structures in the case of a severe earthquake. In this paper, a numerical investigation is carried out to evaluate the seismic demands on old RC waffle plate systems located in southern Spain, in a moderate-to-high seismicity region. A prototype building, designed according to Spanish codes from the 1970´s to 1990´s and current construction practices, was analysed with SAP2000 by using a non-linear static method. The frame model was equipped with user defined hinges based on testing. The low gravity shear ratio and the consideration of punching reinforcement (a usual Spanish practice even when it was not deemed necessary from calculation) leads to a strong column/weak slab behaviour.

Keywords: waffle flat-plate system; seismic resistance, existing building, hinge modelling

1. INTRODUCTION

Waffle flat-slab systems have been widely used in residential and office buildings in southern Europe, even in moderate seismicity regions. Before the 1990´s these systems were designed mainly to deal with gravity loads. Their performance in the event of an earthquake was assessed by means of the simplified equivalent force method, with no specific reinforcing detailing to guarantee ductility. The behaviour of flat-slab buildings exposed to lateral forces has been reported widely. Deserving special attention is the possibility of collapse when neither punching reinforcement nor bottom reinforcement continuity exist, which is indeed a possibility in older flat-slab buildings (Luo et al. 1994, Robertson and Johnson 2006). A clear correlation between gravity shear ratio, interstory drift and punching, based on experimental research, has been reported for interior connections when no punching reinforcement is provided (Hueste and Wight 1999). If the gravity shear ratio does not exceed 0.2, no limitation on drift exists; and when it does not exceed 0.4, punching is produced from 1.5% of drift. When considering lateral loading in a flat-slab frame, the interior slab-column connections are more likely to fail in punching than the exterior connections (Durrani et al. 1995).

A recent survey of construction practices in southern Spain from 1970 to the 1990´s (Benavent et al. 2007) reported that the punching reinforcement was usually introduced in waffle flat-plate buildings even when not necessary. Taking into account the former usual practices and codes, a prototype building was designed and scaled models of interior and exterior slab-column connections were tested. A strong column-weak slab mechanism with no punching failure resulted from the tests of both specimens. Despite favourable results, highly pinched hysteretic load vs. displacement with low energy dissipation ratios were obtained (Cahis et al. 2007). This paper describes further evaluation of previously obtained experimental data, aimed to determine the strength vs. rotation curves on hinges of the exterior and interior connections in waffle flat-plate systems. Hinge models are defined and calibrated from the experimental results, and they are introduced into an effective slab-

width model of one interior frame of the prototype. Non-linear static analysis is performed using SAP 2000 (CSI 2005), and the performance points at service, design and maximum earthquake are obtained by the Capacity Spectrum Method.

2. EXPERIMENTAL BEHAVIOR OF THE COLUMN-SLAB CONNECTIONS

Experimental tests on 3/5 scaled models of one interior and one exterior slab-column connection (IC and EC respectably from now) were performed by cyclic lateral loading until failure was reached. Figure 1 shows the test set-up corresponding to the exterior connection. Gravity loading was simulated by the combination of plate self-weight, sand bags, and an axial load applied to the columns by means of two post-tensioned rods. Both specimens were provided with punching reinforcement, as this was habitual from the seventies to the nineties in southern Spanish constructions (Benavent et al 2007). Further information about the specimens´ characteristics, set-up and preliminary test results are described elsewhere (Benavent et al 2007, Cahis et al 2007). From these experimental tests, moment-rotation models of hinges will be established, with emphasis on measurements from the inclinometers (Fig. 1) and the strain gauges located at the longitudinal upper and bottom reinforcements (Fig. 2). The yielding point, ultimate point (of maximum strength) and failure point will be fixed, and later analysed to determine the moment-rotation hinge model. The yielding displacement point is defined by the secant stiffness at $2Qu/3$ (Pan and Moehle, 1989), and failure is assumed to occur when the lateral capacity dropped below 0.8 Q_u (Park, 1986). Figure 3 shows the load-deformation curves for both connections with these significant points.

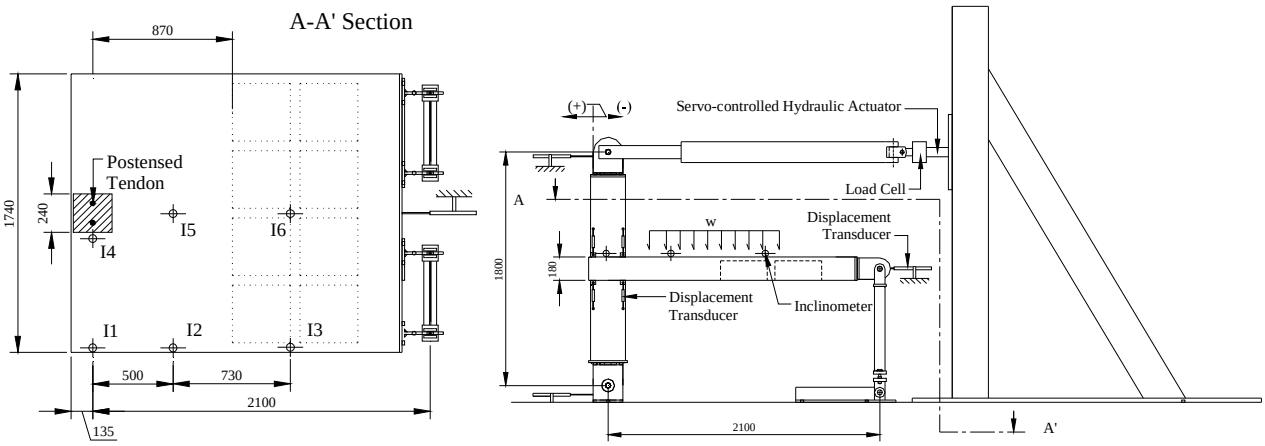

Figure 1: Loading and instrumentation set-up of the exterior slab – column connection model

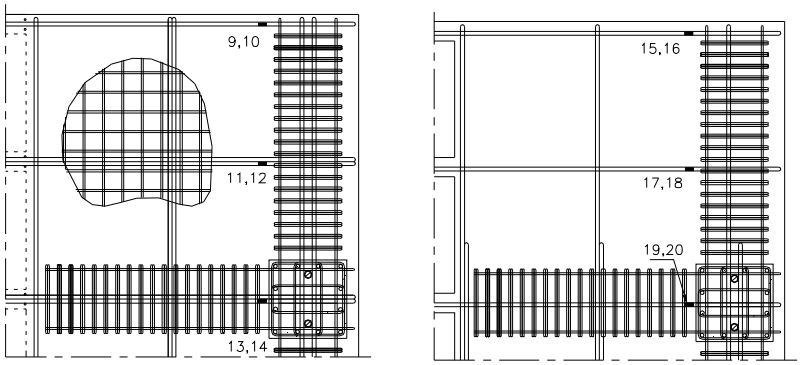

Figure 2: Location of strain gauges: a) upper longitudinal reinforcement, b) bottom longitudinal reinforcement

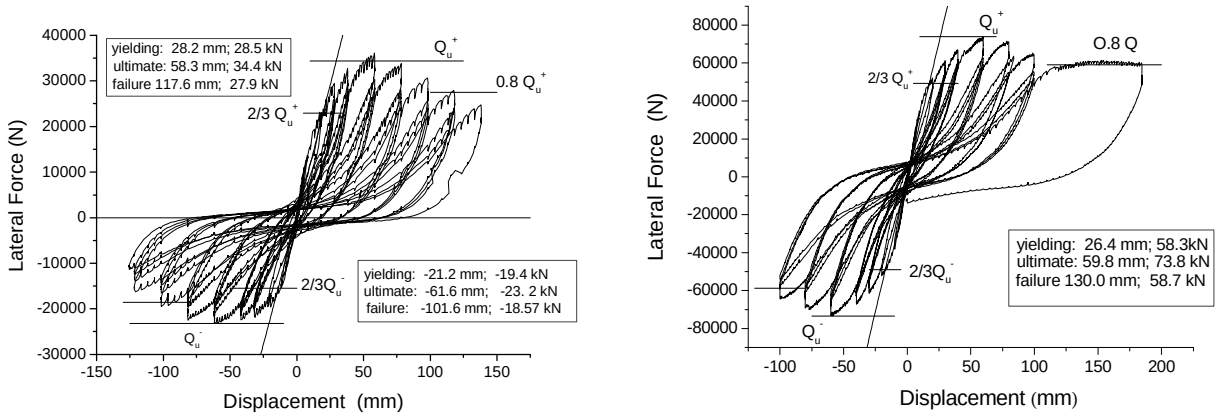

Figure 3: Lateral force–displacement curve: a) exterior connection, b) interior connection

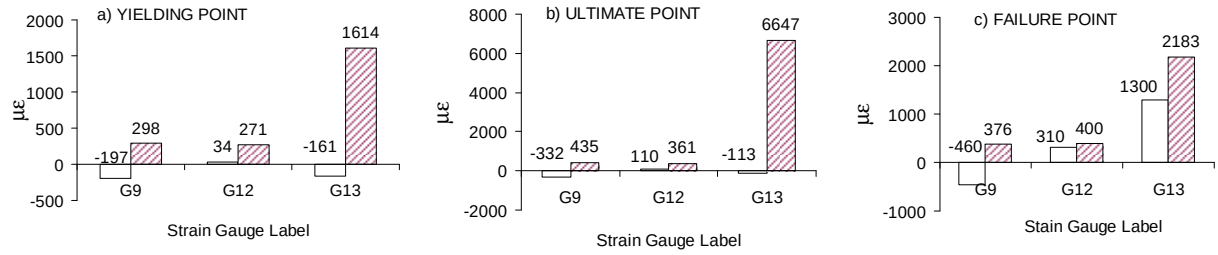

Figure 4: Strain distribution of the upper reinforcement of EC in negative curvature (shared) compared with the strain distribution in the previous maximum positive curvature

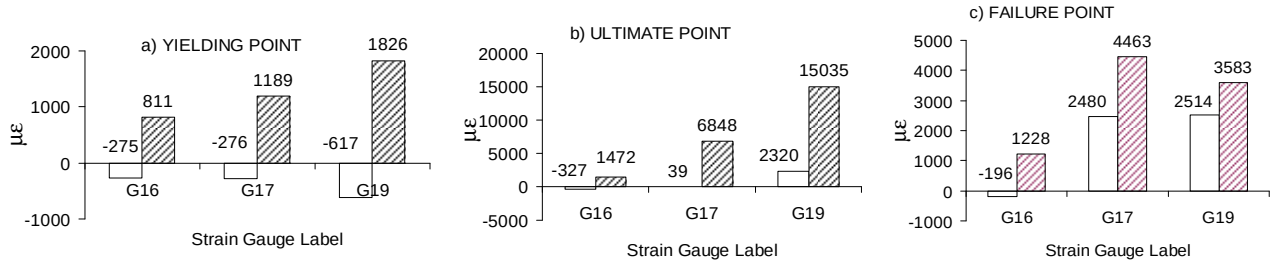

Figure 5: Strain distribution of the bottom reinforcement of EC in positive curvature (shared) compared with the strain distribution in previous maximum negative curvature

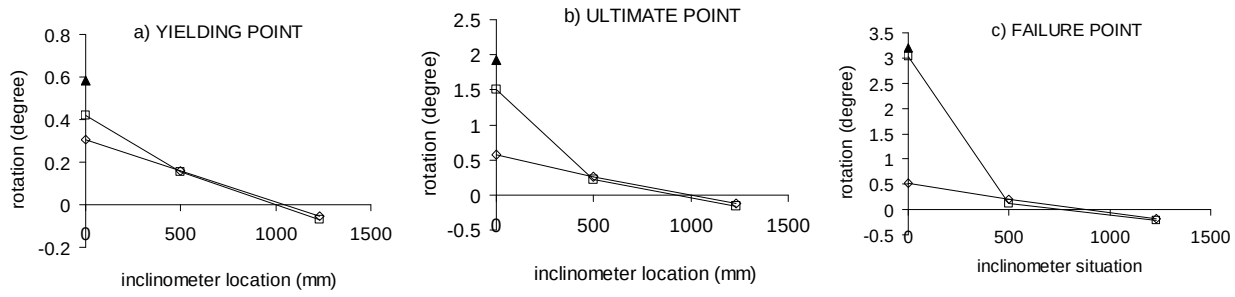

Figure 6: Measures of rotation of the inclinometers in EC model in hinge positive curvature: ▲ Column rotation, ◊ edge slab inclinometers, □ central slab inclinometers

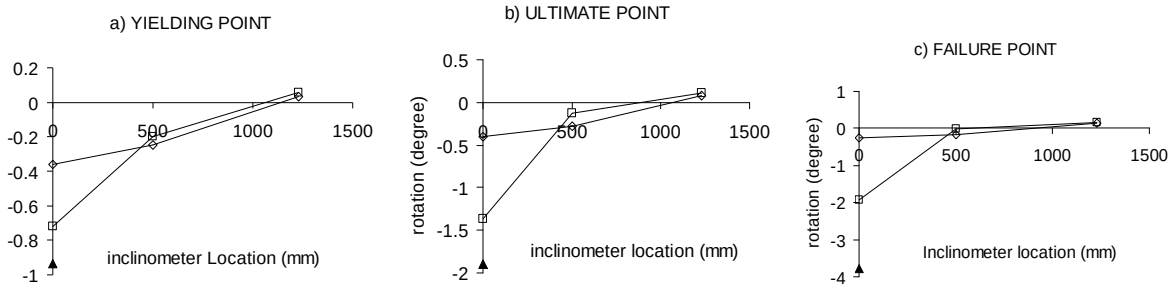

Figure 7: Measures of rotation of the inclinometers in EC model in hinge negative curvature: ▲ Column rotation, ◊ edge inclinometers, □ central slab inclinometers

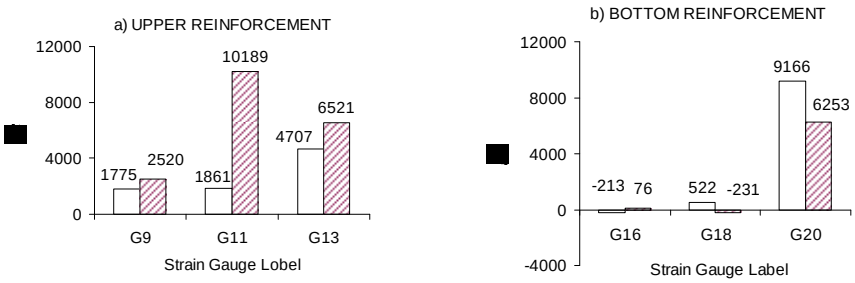

Figure 8: Strain distribution of longitudinal reinforcement at the failure point

The moment strength of the exterior connection can be obtained from $M_f + 2T$, where M_f is the moment of the effective slab-width and T is the torsional strength of the spandrel beam (Luo et al. 1994, Durrani et al. 1995). The yielding point, at 1.1 % of the interstory drift for bottom bars and 1.6 % for upper bars (in positive and negative curvatures, respectively), produced first yielding in the longitudinal bars anchored directly to the column due to flexure (Figs. 4a and 5a). Maximum capacity load (ultimate point) accounts for nearly 3.3% of the interstory drift, both in positive and negative displacements, when inclinometer 1 obtains the maximum rotation from spandrel beam torsion (Figs. 6a, 6b, 7a and 7b). At this point rotation decreases, because of degrading of the spandrel beam (Figs. 6c and 7c). The post-ultimate behaviour is determined by the torsion cracking and the degradation of the anchoring of longitudinal bars situated in the effective slab-width due to spandrel beam cracking. At the failure point, the strain gauges of the bars directly anchored to the column measured high positive deformation, but also important positive strains in the previous (different) sign displacement because of a loss of adherence of the anchorage (Fig. 4c and 5c). The strain gauges located on the outer longitudinal bars registered almost 80% of the strain measured at the ultimate point. The interior connection reaches the maximum strength at 3.3% of the interstory drift. The failure point is determined by the loss of adherence of the bottom reinforcement, as indicated by the strain gauge values of Figure 8b. At this point, the upper reinforcement still works, as reflected in the strain gauge measurements (Fig. 8a) and the load displacement curve (Fig. 3b).

3. HINGE MODELLING

The cross section of the effective beam for the exterior connection has been defined as trapezoidal. For the upper dimension the ACI 308-05 (ACI 2005) proposal, $c1+3h$, was assumed, which gives similar results as the strut-and-tie mechanism. But in the case of the bottom reinforcement, the strut-and-tie mechanism and other experimental results (Luo et al. 1994, Durrani et al. 1995, Dovich and Wight 2005) suggest that $c1+c_2$ is more realistic. The strength of the exterior connection can be determined by the sum of the flexure capacity of the effective beam and the torsion strength of the lateral column spandrel beams, M_f+2T. For the interior

connection, the ACI 318-05 proposal (*c1+3h* of effective beam width and Mf/γ_f as flexural moment, with γ_f=0.6 for square columns) can be assumed to predict the ultimate capacity (Benavent et al. 2008).

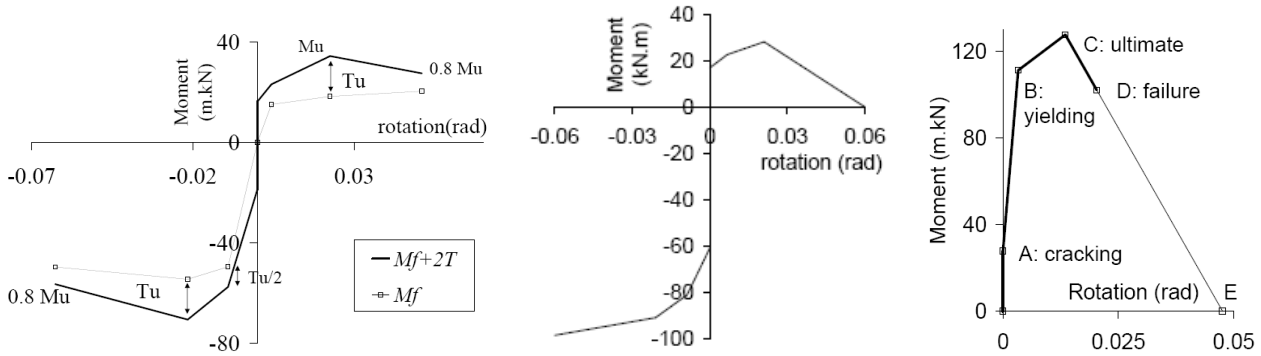

Fig. 9: Hinge moment – rotation curve. a) EC slab-column connection, b) IC slab-column connection, c) IC Column hinge

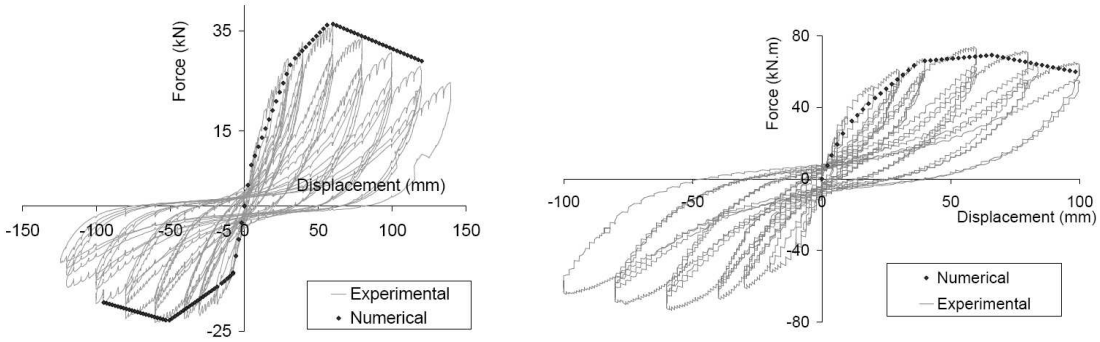

Fig. 10: Lateral load versus displacement of models: a) EC, b) IC

The experimental appreciation of the failure of the spandrel beam by torsion in the EC, and the adherence failure of bottom reinforcement in the IC, were used to construct the M-O hinge curve, seen in Figs. 9a and 9b. The ultimate and degrading rotations were obtained from experimental relative rotation between inclinometers 4 and 5 (Fig. 1). The moment-curvature of the effective slab-width section was obtained using the reinforced concrete sectional analysis program Response 2000 (Bentz and Collins 2000), and the curvature was transformed into rotation through the experimental adjusted expressions of Panagiotakos and Fardis (2001), adapted to the experimental results of the waffle slab tested connections. The hinge moment-rotation of the columns was defined as a multilinear function (Fig. 9c) with different significant points: a) cracking, b) yielding, c) ultimate, d) failure, e) loss of lateral capacity. The failure point was defined as moment dropping below 0.8 of the ultimate moment. The Elwood and Moehle (2005) expression was used to define total deformation at point "E". To obtain the rotation of hinge θ, at the yielding and ultimate points, the expression by Panagiotakos et al. (2001) is adapted:

$$\theta = \phi \frac{L_s}{3} + \theta_s + a_{sl} \frac{0.25\varepsilon d_b f_y}{(d-d')\sqrt{f_c'}} \qquad (3.1)$$

where ϕ is the section curvature, L_s is the shear span (M/V), θ_s is the shear deformation, and coefficient a_{sl} equals 1 if slippage of longitudinal steel from its anchorage zone beyond the end section is possible, or 0 if not; ε is the strain of tension reinforcement, d_b and f_y are respectively the diameter and the yield strength of the longitudinal steel reinforcement, *d-d'* is the distance between tension and compression reinforcement, and f_c' is the compressive strength of concrete. To obtain the shear deformation, at the yielding and the ultimate points, the models proposed by Sezen (2008) were used. Results with the expression 3.1 and Sezen models were then compared to the experimental deformations of columns with light transverse reinforcement (Sezen and Moehle 2006) and sufficient correlation was obtained.

The tested specimens (Cahis et al. 2007) were analized by a non-linear pushover with SAP 2000 (Computers

and Structures Inc. 2005). Hinges were introduced at the end of the columns and the beams. A midspan width of $2c_1+l_1/3$ (Hwang and Moehle 2000) was considered, and respective reductions of 0.7 and 1/3 were applied to the gross section stiffness of supports and to effective slab-width elements (Vanderbilt and Corley, 1983). Figures 10a and 10b reveal a good approximation between the skeleton curves of the experimental tests and the numerical results.

4. NON-LINEAR STATIC ANALYSIS OF A PROTOTYPE OF BUILDING

Figure 11 shows an interior frame of the prototype of building that has been numerically analized. Reinforcement of the connections corresponds to the effective slab-width, and has been calculated on the basis of former Spanish code. The same considerations of the previous section about cracking and effective slab-width of structural elements have been used. Further information on the building prototype can be found in the literature (Benavent et al. 2007).

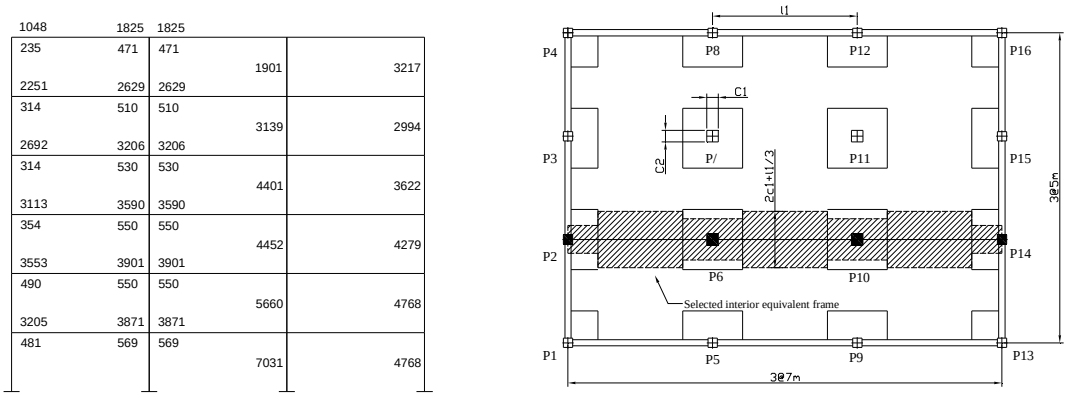

Fig. 11: Interior equivalent frame: a) reinforcement values (mm^2), b) effective slab-width

Table 4.1.: Main parameters of the performance points

Performance Point	*V/W* (base shear ratio)	Max. drift (%)	Max. I.D. (%)	Effective period (s)	Effective damping (%)
S.E.	0.107	0.81	0.98	1.78	6.4
D.E.	0.132	1.42	1.74	2.13	11.4
M.E.	0.136	2.01	2.32	2.52	15.5

The non-linear pushover of the interior frame, bearing in mind user defined hinges and P-Delta effects, was calculated with SAP 2000 v8; the performance point was determined for the Service, Design and Maximum Earthquakes using the Capacity Spectrum Method (CSM). An inherent damping coefficient β of 5% and a "Structural Behavior Type C" (the hysteretic loops are highly pinched) were inferred (ATC-40). Departing from a PGA value of 0.23g (the basic acceleration of city of Granada, Spain) for the Design Earthquake, coefficients of 0.5 and 1.5 were applied to determine the SE and the ME. The main data regarding performance points and hinge distribution in the frame are shown in Table 4.1 and Figure 12, respectively. The Service Earthquake produced some hinges with moderate yielding, mainly in the exterior connections, owing to positive moment. Maximum interstory drift was near 1%, meaning that damage in structural and also non-structural elements was to be expected. The Design Earthquake produced new hinges, mainly situated at the end of beams and due to positive moments, with low-to-moderate yielding. The Maximum Earthquake, in turn, pushed the structure close to collapse. Some of the existent slab hinges with positive curvature nearly collapsed, and new slab hinges on negative moments underwent significant yielding. The collapse of the structure, according to pushover analysis, would be the result of failure of some exterior connections with negative moment and interior connections because positive moments and adherence failure of the bottom reinforcement.

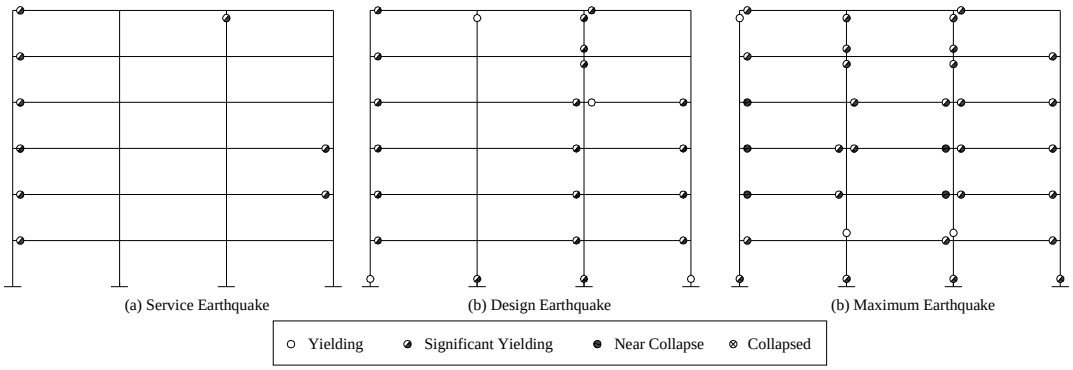

Figure 12: Distribution of hinges in the equivalent frame: a) SE, b) DE, c) ME

5. CONCLUSIONS

Experimentally based moment-rotation hinge models, for interior and exterior waffle slab-column connections, are herein defined for use in effective beam frame analysis. The test specimens were provided with punching reinforcement, a usual practice in southern Spain during the decades of the 1970´s, 80´s and 90´s for waffle flat-plate frames. Torsion cracking in the exterior column spandrel beams and adherence failure of bottom reinforcement in the interior connections can be considered as the main degrading factors. The effective slab-width and strength models proposed by ACI 318-05 present good correlation with experimental results in the interior connections. In the case of the exterior connection, meanwhile, a trapezoidal effective cross section was considered, c_1+3h and c_1+c_2 being the upper and bottom dimensions, respectively. A strength model for exterior connections accounting for the flexure of the effective slab-width as well as the torsion capacity of the edge spandrel beams is calibrated based on experimental data. The hinge models obtained and presented here appear to accurately reproduce the experimental load-deformation curves derived from tests, thus proving useful for RC waffle flat-plate building assessment. A pushover curve taking into account hinge non-linearities and P-Delta effects has been obtained for a waffle flat-plate equivalent frame; the performance point in the Service, Design and Maximum Earthquakes using the Capacity Spectrum Method have been calculated. Strong column-weak slab behaviour was appreciated until reaching collapse, slightly beyond the Maximum Earthquake performance point. Before collapse, which occurred at 2.3% of maximum displacement, the interstory drift was almost uniformly distributed throughout the height of the frame.

ACKNOWLEDGEMENTS

This research received support from the Spanish Government (Ministerio de Fomento) within *Programa Nacional de Construcción* 2004-2007 (project number 2004/39–80020/A04). The authors wish to thank J. Mata-Vico and J. Gil-Villaverde of the University of Granada, and S. Kishiki of the Tokyo Institute of Technology, for their valuable assistance before and during the tests.

REFERENCES

ACI Committee 318 (2005). Building Code requirements for reinforced concrete, American Concrete Institute, Farmington Hills, Mich.

ATC 40 (1996). Seismic evaluation and retrofit of concrete buildings, Applied Technology Council, Redwood City, CA.

Benavent A., Cahis, X. and Catalan, A. (2007). Capacidad sismorresistente de estructuras de hormigón armado

con forjados reticulares. Primera parte. *Proceedings on 3rd NSEC*, Girona, Spain.

Benavent A., Cahis X. and Catalan A. (2008), "Seismic behavior of interior connections in existing waffle-flat-plate structures", *Engineering Structures* (in press).

Bentz E.C. and Collins M.P. (2000). Response 2000-Reinforced Concrete Sectional Analysis – version 1.05, University of Toronto, Canada.

Cahis X., Benavent, A. and Catalan, A. (2007) Capacidad sismorresistente de estructuras de hormigón armado con forjados reticulares. Segunda parte: ensayos". *Proceedings on 3rd NSEC*, Girona, Spain.

Computers and Structures Inc. (2005); SAP2000-Integrated Software For Structural Analysis & Design, non-linear version 8.3.3, Berkeley, CA.

Dovich L.M. and Wight J.K. (2005). Effective slab width model for seismic analysis of flat slab frames. *ACI Structural Journal* **102:6**, 868-875.

Durrani A.J. Du Y. and Luo Y.H. (1995). Seismic Resistance of Nonductile slab-column connections in existing flat-slab buildings. *ACI Structural Journal* **92:4**, 479-487.

Elwood, K.J. and Moehle, J.P (2005). Axial capacity model for shear-damaged columns. *ACI Structural Journal* **102:4**, 578-587

Huang S. J. and Moehle J.P. (2000). Models for laterally loaded slab-column frames. *ACI Structural Journal* **97:2**, 345-351

Hueste, M.D. and J.K. Wight (1999). A Nonlinear Punching Shear Failure Model for Interior Slab-Column Connections. *ASCE Journal of Structural Engineering* **125:9**, 997-1008.

Luo Y.H. Durrani A.J. and Conte J.P. (1994). Equivalent frame analysis of flat-plate buildings for seismic loading, *ASCE Journal of Structural Engineering* **120:7**, 2137-2155.

Pan A. and Moehle J. P. (1989). Lateral displacement ductility of reinforced concrete flat plates. *ACI Structural Journal* **80:3**, 250-257.

Panagiotakos T.B. and Fardis M.N (2001). Deformations of reinforced concrete members at yielding and ultimate". *ACI Structural Journal* **98:2**, 135-147.

Park, R. (1986). Ductile design approach for reinforced concrete frames. *Earthquake Spectra* 2:3, 565-619.

Roberson I. and Johnson G. (2006). Cyclic lateral loading of nonductile slab-column connections. *ACI Structural Journal* **103:3**, 356-364.

Sezen H. and Moehle J.P. (2006). Seismic tests of concrete columns with light transverse reinforcement. *ACI Structural Journal* **103:6**, 842-849.

Sezen H. (2008). Shear deformation model for reinforced concrete columns. *Structural Engineering and Mechanics* **28:1**, 39-52

Vanderbilt M.D. and Corley W.G. (1983). Frame Analysis of Concrete Buildings. *Concrete International, American Concrete Institute* 33-43